Induction of *Ucp2* expression in brain phagocytes and neurons following murine toxoplasmosis: An essential role of IFN-γ and an association with negative energy balance

Denis Arsenijevic [a,1], Sébastien Clavel [b,1], Daniel Sanchis [c], Julie Plamondon [b], Quingling Huang [b], Daniel Ricquier [c], Laurie Rouger [b], Denis Richard [b,*]

[a] *Department of Medicine, Division of Physiology, University of Fribourg, Ch. Du Musée 5, Fribourg, Switzerland*
[b] *Centre de recherche de l'Hôpital Laval, 2725, Chemin Sainte-Foy, Sainte-Foy (Québec), Canada G1V 4G5*
[c] *Centre National de la Recherche Scientifique UPR 9078, Faculté de médecine Necker-Enfants Malades, Paris, France*

Abstract

A model of murine toxoplasmosis was used to study cellular and temporal expression of uncoupling protein-2 (*Ucp2*) in the brain. *In situ* hybridization indicated that *Ucp2* was located in neurons. Nuclei structures involved in energy balance, in particular the nucleus of the solitary tract (NST), was shown to have a positive association between negative energy balance and *Ucp2* levels. Infection-induced *Ucp2* expression colocalized mainly with microglial cells, but also with infiltrating macrophages and neutrophils in the brain, which was evident from day 9 post-infection. Using cytokine knockout mice we demonstrate that microglial *Ucp2* induction in the brain was largely dependant on interferon-γ, but not interleukin-6 or tumour-necrosis-factor-α in response to infection. In summary, this study shows that *Ucp2* is regulated in a different manner in neurons than in microglia/phagocytes following infection. Our study indicates that an association exists between negative energy balance and neuronal *Ucp2* levels in the NST, in particular.

Keywords: Uncoupling-protein-2; Toxoplasmosis; Brain; Neuron; Microglia; Interferon-gamma

1. Introduction

Uncoupling proteins 1, 2 and 3 form a subfamily of mitochondrial carrier proteins. *Ucp1* is the archetypical uncoupling protein. It is found in the inner membrane of the mitochondrion, where it uncouples fuel oxidation from ATP synthesis by dissipating the proton gradient that builds up across the inner membrane during the transport of electrons through the respiratory chain. In the presence of an active *Ucp1*, the proton motive force is not used for ATP synthesis, but is dissipated as heat (Nichols and Locke, 1984). In contrast to *Ucp1*, which is specifically expressed in brown adipose tissue, *Ucp2* mRNA has been detected in a large spectrum of mammalian tissues (Fleury and Sanchis, 1999), where its function largely remains to be resolved. Instead of what was initially anticipated (Fleury et al., 1997), *Ucp2* does not seem to be critical in energy balance under normal conditions. Accordingly, studies carried out in *Ucp2* knockout (KO) mice have shown that these mice exhibit a normal thermogenic response to cold (Arsenijevic et al., 2000). *Ucp2* expressed in peripheral tissue is modulated by numerous conditions and treatments (Argyropoulos and Harper, 2002; Ricquier and Bouillaud, 2000) but its role is still a matter of debate. However, it has been suggested that *Ucp2* is a negative regulator of insulin secretion in pancreatic islet by decreasing ATP levels (Zhang et al., 2001). A study by our group also proposed that *Ucp2* may have functions in immunity and reactive oxygen species (ROS) production (Arsenijevic et al., 2000). When challenged with an infection, *Ucp2* KO mice were

* Corresponding author. Institut Universitaire de Cardiologie et de Pneumologie, Hôpital Laval, 2725, Chemin Sainte-Foy, Sainte-Foy (Québec), Canada, G1V 4G5.
   E-mail address: Denis.Richard@phs.ulaval.ca (D. Richard).
[1] These authors contributed equally.

more resistant to *Toxoplasma gondii* infection. This was explained by a larger amount of ROS produced by their macrophages and enhanced elimination of the microbe. An important *in vitro* study also showed that *Ucp2* may be regulated by superoxide production (Echtay et al., 2002).

In the murine brain, *Ucp2* is expressed in specific regions as well as in ventricle-associated areas, these cells being predominantly neuronal populations of subcortical regions that are involved in the central regulation of autonomic, endocrine, and metabolic processes (Richard et al., 1998). *Ucp2* has been studied in pathophysiological models such as ageing (Mizuno et al., 2000), epilepsy (Clavel et al., 2003; Diano et al., 2003; Sullivan et al., 2003), Parkinson's disease (Andrews et al., 2005), ischemia (de Bilbao et al., 2004; Mattiasson et al., 2003) and brain trauma (Mattiasson et al., 2003). The currently proposed view concerning *Ucp2* action is that it may act as a sensor of the redox state and may then decrease subsequent ROS production. However, it is important to acknowledge that brain degenerative processes are also generally accompanied by the activation of the innate immune system represented by activated astrocytic and phagocytic microglial cells. This activation may also be involved in driving the *Ucp2* expression. Interestingly, cytokines and lipopolysaccharide (LPS) injections are well known to alter *Ucp2* in a variety of tissues (Busquets et al., 2001; Cortez-Pinto et al., 1998; Faggioni et al., 1998; Masaki et al., 1999; Yu et al., 2000) including the brain. Proposed functions for the *Ucp2* following acute immune challenge include the increased in energy expenditure and a role in protecting cells against oxidative stress.

Toxoplasmosis affecting the central nervous system is now one of the leading causes of death among AIDS patients (Holliman and Greig, 1997). *T. gondii* is an obligate intracellular parasite capable of infecting nearly all warm-blooded animals. We initially used this infection because this parasite greatly affects energy balance and induces phases specific for hypermetabolism and anorexia in mice in a well characterized fashion (Arsenijevic et al., 1997). Parasite cysts formation is common in the brain during the course of toxoplasmosis where cellular immune responses are restricted due to the blood brain barrier and low expression of the major histocompatibility complex antigens (Daubener and Hadding, 1997). Brain inflammation in the chronic phase of infection is caused by rupture of cysts. The earlier part of the infection (day 9 and onward) is accompanied by immune cell infiltration of the brain by macrophages, monocytes, neutrophils, B cells, CD4+ and CD8+ T cells. Moreover, the main defence against *T. gondii* is mediated by natural killer (NK), T-cells and macrophages. The NK and T-cells produced IFN-γ, which is a major component involved in the defence against *T. gondii* in brain tissue (Chao et al., 1993; Yap and Sher, 1999). Macrophages and lymphocytes also produced interleukin-6 (IL-6) or tumor-necrosis-factor-α (TNF-α), which are involved in the immune responses against this parasite (Daubener and Hadding, 1997).

In a previous study, we studied the immune defense and ROS production of *Ucp2* KO mice to *T. gondii* infection. However, the role of immune cells and their cytokines in driving *Ucp2* expression regulation, following infection, is still unknown. In order to study the brain regulation of *Ucp2*, the objectives of the present study were (i) to identify cells expressing *Ucp2* before and after infection in order to assess the effect of infection on *Ucp2* in brain cell subgroups such as neurons and microglia, (ii) to determine if *Ucp2* may be associated with negative energy balance observed following infection by studying *Ucp2* expression in a few nuclei involved in energy balance — the area postrema (AP), nucleus solitary tract (NST), ventromedial hypothalamic nucleus (VMH) and arcuate nucleus (ARC), (iii) to delineate the role of immune cells infiltration in driving *Ucp2* expression by investigating the temporal and associated cellular expression of this gene in both acute and chronic phases of the *T. gondii* infection and (iv) to examine whether cytokines such as TNF-α, interferon -γ (IFN-γ) and IL-6, induced in the course of *T. gondii* infection, may be involved in *Ucp2* regulation.

2. Materials and methods

2.1. Animals and treatment

Male Swiss Webster (CFW) mice (Charles River, Canada) of 4–6 weeks of age were used for all the experiments. Cytokine deficient mice used were IFN-γ KO (BALB/c-Ifng^{tm1Ts}), TNF-α KO (C57BL/6-TNF^{tm1Gkl}) and IL-6 KO (C57BL/6J-IL6^{tm1kopf}) (Jackson Laboratories, Bar Harbour, ME,USA). The mice were housed individually in polycarbonate cages, kept at room temperature with a 12:12 h light dark cycle and had free access to tap water and standard laboratory chow diet. Mice were injected intraperitoneally with 10 cysts of the Me49 strain of *T. gondii* (obtained from Dr L.L. Johnson, Trudeau Institute, Saranac Lake, NY, USA) and the brains were collected. All mice were cared for and handled according to the Canadian guide for the Care and Use of Laboratory Animals. The present protocol was approved by our institutional animal care committee.

2.2. Northern blot

Mice which were chronically infected for 28 days and which comprise Gainers (G), Non-Gainers (NG) and non-infected controls ($n=3$ per group) were used to determine central *Ucp2* mRNA. Mice were deeply anesthetized with 0.3–0.5 ml of a mixture containing 40 mg/ml of ketamine and 2 mg/ml xylazine. Without delay they were intracardially perfused with ice-cold isotonic saline. At the end of the perfusion the whole brains were quickly dissected out and frozen. Total RNA was prepared as described before (Chomczynski and Sacchi, 1987). Northern blot analyses were performed using the mouse *Ucp2* cDNA labeled with ^{32}P under standard conditions. Similar amount of total RNA (20 μg) was used in every lane.

2.3. In situ hybridization histochemistry

In situ hybridization histochemistry was used to localize *Ucp2* mRNA on tissue sections taken from the olfactory bulb to the brainstem in non-infected control mice and infected mice on days 1, 3, 9, 14 and 28 post-infection. Note that on day 28 after infection mice consist of 2 subgroups the G and NG. The protocol used was largely adapted from that described by
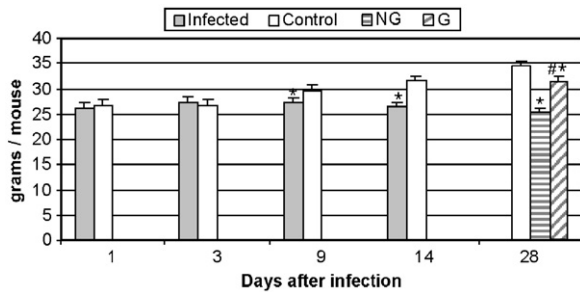
Fig. 1. A, Body weight in mice infected (i.p.) with 10 cysts of *Toxoplasma gondii* (Me49 strain). Values are presented as mean±SEM for the various group (*n*=6), and abbreviated as follows: G = Gainers and NG = Non-Gainers. *Indicates a significant difference when compared to Control group (*p*<0.01). #Indicated a significant difference when comparing NG to G (*p*<0.05).

Simmons (Simmons et al., 1989). Briefly, one out of every 5 brain sections were mounted on to poly-L-lysine coated slides and allowed to desiccate overnight under vacuum. The sections were then successively fixed for 20 min in paraformaldehyde (4%), digested for 30 min at 37 °C with proteinase K (10 µg/ml in 100 mM Tris–HCl containing 50 mM EDTA, pH 8), acetylated with acetic anhydride (0.25% in 0.1 M trietholamine, pH 8) and dehydrated through graded concentrations (50, 70, 95 and 100%) of alcohol. After vacuum drying for at least 2 h, 90 µl of hybridization mixture, which contains an antisense ^{35}S labeled cRNA probe (10 million cpm/ml), were spotted on each slide. The slides were sealed under a coverslip and incubated overnight at 60 °C in a slide warmer. The next day, the cover slips were removed and the slides rinsed four times with 4X SSC (0.6 M NaCl, 60 mM sodium citrate buffer, pH 7). They were digested for 30 min at 37 °C with RNAse A (20 µg/ml in 10 mM Tris–500 mM NaCl containing 1 mM EDTA, washed in descending concentrations of SSC (2×, 10 min; 1×, 5 min; 0.5×, 5 min; 0.1×, 30 min at 60 °C), and dehydrated through graded concentrations of alcohol. After a 2-hour period of vacuum drying, the slides were exposed on an X-ray film (Eastman Kodak, Rochester, NY) for 24 h. Once removed from the autoradiography cassettes, the slides were defatted in xylene and dipped in NTB2 nuclear emulsion (Eastman Kodak). They were exposed for 7 days, before being developed in D19 developer (Eastman Kodak) for 3.5 min at 15 °C and fixed in rapid fixer (Eastman Kodak) for 5 min. Finally tissues were rinsed in running distilled water for 1 to 2 h, counterstained with thionin (0.25%), dehydrated through graded concentrations of alcohol, cleared in xylene and coverslipped with DPX.

2.4. Antisense (^{35}S)-labeled cRNA probes

The *Ucp2* cRNA probe was generated from the 945 bp *Eco*R1 fragment of a mouse *Ucp2* cDNA subcloned into a pSELECT vector (Promega Inc., Lyon, France), which was linearized with *Sac*I and *Knp*I (Pharmacia Biotech Canada, Inc., Baie d'Urfè (Qc), Canada) for sense and antisense probes, respectively. The radioactive riboprobes were synthesized by incubating 250 ng of the linearized plasmid into a solution containing 10 mM NaCl, 10 mM dithiothreitol, 6 mM MgCl, 40 mM Tris (pH 7.9), 0.2 M ATP/GTP/CTP, alpha (^{35}S)-UTP,

40 U RNasin (Promega, Madison, WI) and 20 U SP6 and T7 RNA polymerase for sense and antisense probes, respectively, for 60 min at 37 °C. The DNA templates were treated with 100 ml of a DNAse solution (1 ml DNAse, 5 ml of 5 mg/ml tRNA and 94 ml of 10 mM Tris/10 mM MgCl$_2$). The preparation of the riboprobes was completed through a phenol-chloroform extraction and ammonium acetate precipitation. The specificity of the antisense riboprobe was confirmed by the absence of a positive signal in brain sections hybridized with the sense probe (not shown).

2.5. Combination of immunohistochemistry with in situ hybridization

Immunocytochemistry was combined with *in situ* hybridization histochemistry to determine the phenotype of the cells that express *Ucp2* mRNA in the mouse brain after infection of *T. gondii* on days 1, 3, 9, 14 and 28 post-infection. The following antibodies were obtained from Cedarlane (Hornby, Ontario, Canada) unless otherwise stated and were used to detect subtypes of immune cells: macrophage–monocytes and microglial cells were stained using the anti-F4/80 antibody (1:500), microglial cells by the antibody directed against Iba-1 molecule (1:500, gratefully provided by Dr. Yoshinori Imai); anti-neutrophils (1: 500); natural killer cells with the anti-asialo GM1 antibody (1:500); B cells by pan B cell marker CD45R Ly5 antibody (1:2500); leukocyte common antigen CD45 (1:500); T-cell subset by CD4 (1 :100) and CD8 (1 :100) antibodies; and endothelial cells were stained using von Willabrandt factor (1:30000). Astrocytes were stained using the mouse anti-glial fibrillary acidic protein antibody, purchased at Chemicon International Inc. (CA, USA) (1:1200). Brain sections were
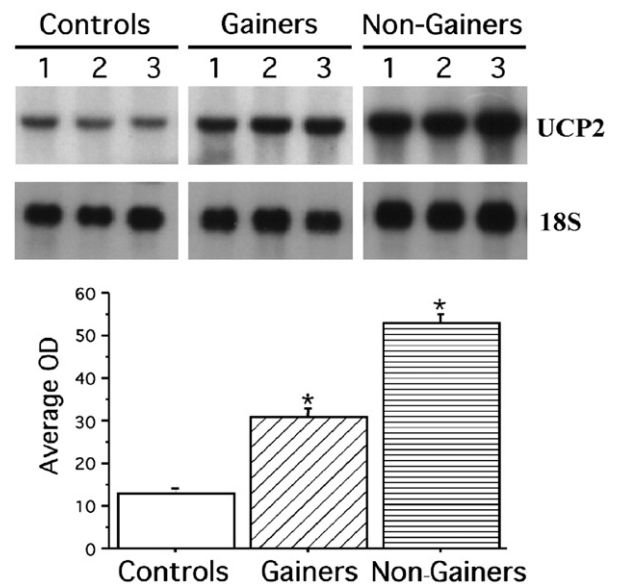

Fig. 2. Northern blot analysis of *Ucp2* mRNAs in the brain of controls, infected Non-Gainers and infected Gainers mice. A, Top panel, an autoradiograph with uncoupling protein 2 mRNA is shown. Bottom panel, constitutively expressed RNA (18S) on the same blot. B, PhosphorImage data, *Ucp2* signal was normalized for 18S RNA expression in the same sample. Results are mean S.E., *n*=3, *p*<0.001 NG and G *vs* controls.
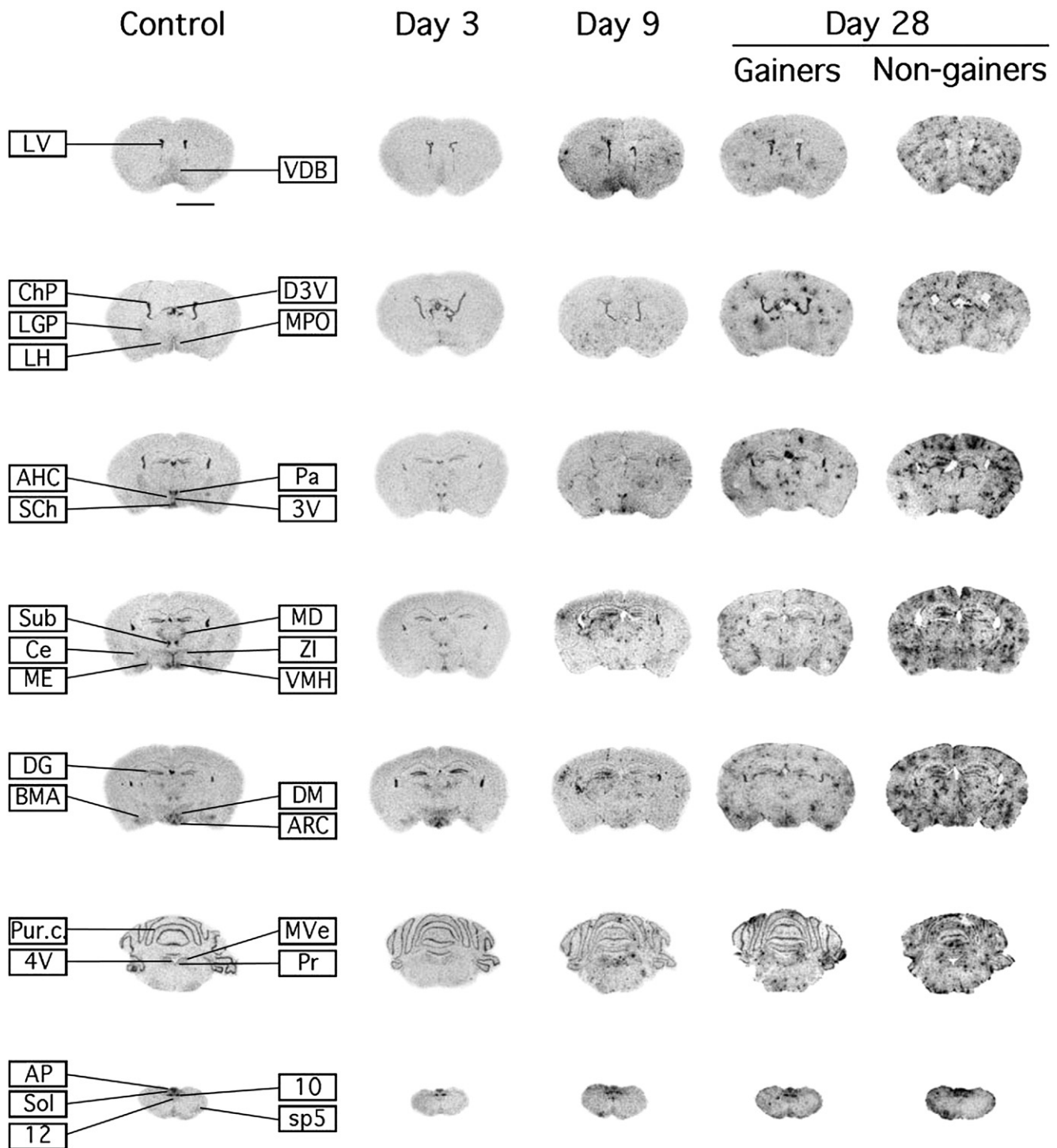
Fig. 3. Rostrocaudal distribution of *Ucp2* mRNA in the mouse brain under basal condition and following an i.p. injection with 10 cysts of the Me49 strain of *Toxoplasma gondii* in the brain of Swiss Webster mice. Animals were killed 3, 9 and 28 days after i.p. infection. These rostrocaudal sections (Scale bar: 25 µm) exhibit a positive signal on X-ray film on various structures of the brain. The pictures represent the X-ray film autoradiograms of coronal brain sections representative of the group (*N* = 4) that were hybridized with an antisense riboprobe complementary to mouse *Ucp2* mRNA. Each presented section approximately corresponds to the same rostrocaudal level for the groups, which allows the comparison within distribution.

first processed for immunocytochemical detection of one of the previous antibodies using a conventional avidin–biotin–immunoperoxidase method. Briefly, brain slices were washed in sterile 50 mM potassium PBS (KPBS) that was treated with diethylprocarbonate water. They were then incubated overnight at 4 °C with one of the previous mentioned antibodies in KPBS (50 mM) with heparin (0.25%), Triton X-100 (0.4%) and BSA (2%). Following incubation at 4 °C with the first antibody, the brain slices were rinsed in sterile KPBS and incubated with a mixture of KPBS, Triton X-100, heparin, a biotinylated
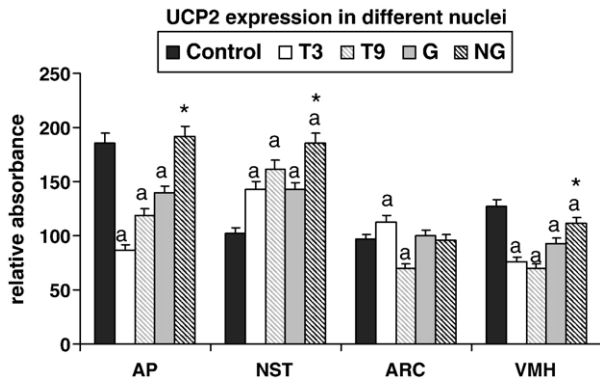
Fig. 4. *Ucp2* expression in the area postrema (AP), nucleus solitary tract (NST), ventromedial hypothalamus nuclei (VMH) and arcuate nucleus (ARC) on days 3, 9 and 28 after *Toxoplasma gondii* infection, note that on day 28 infected mice consist of two subgroups the Gainer (G) and the Non-Gainers (NG). The levels of *Ucp2* mRNA was determined as described in the methods section on brain slices by densitometry scans on the respective nuclei, $N = 4$ mice per group. Note that "a" indicates that there was a significant difference ($p < 0.001$) when compared to the control group, * indicates that there is a significant difference ($p < 0.001$) comparing the NG to G group.

appropriated second antibody for 60 min. Sections were then rinsed with KPBS and incubated at room temperature for 60 min with an avidin–biotin–peroxidase complex (Vectasain ABC Elite Kit; Vector labs., Burlingame, CA). After several rinses in sterile KPBS, the brain slices were allowed to react in a mixture containing sterile KPBS, the chromagen 3,3′-diaminbenzidine tetrahydrochloride (DAB, 0.05%) and 1% hydrogen peroxide. Thereafter, tissues were rinsed in sterile KPBS, mounted onto poly-L-lysine-coated slides, dessicated overnight under vacuum, fixed in paraformaldehyde (4%) for 3 min, and digested for 30 min at 37 °C with proteinase K (10 mg ml in 100 mM Tris HCL, pH 8.0, and 50 mM EDTA). Pre-hybridization, hybridization, and post-hybridization steps were performed as described above except for the dehydration step, which was shortened to avoid decolorization. After vacuum drying for 2 h, sections were exposed on X-ray film, defatted in xylene, and dipped in the NTB2 nuclear emulsion. Slides were exposed for 7 days, developed in D19 developer for 3.5 min at 15 °C, and fixed in rapid fixer for 5 min. Thereafter, tissues were rinsed in running distilled water for 1–2 h, rapidly dehydrated through graded concentrations of alcohol, cleared in xylene, and coverslipped with DPX.

3. Results

3.1. Body weight, food intake and energy expenditure following infection

Fig. 1 illustrates the body weight changes following infection. We previously characterized our model (data not shown, Arsenijevic et al., 1997) and showed that all infected mice were hypermetabolic from day 1 following the infection. After 7–14 days, all mice exhibited a weight loss, which was associated with anorexia and hypermetabolism. After day 14, mice started to stabilize their body weight and food intake. Subsequently, the infected mice were classified as 'Gainers' (G)

if they showed a regain in body weight after infection-induced cachexia or 'Non-Gainers' (NG) if they showed no regain after the acute phase of infection. In the chronic phase on day 28, the NG remained hypermetabolic and anorexic, while G were not hypermetabolic but anorexic. Both G and NG maintained stable body weight and food intake in the chronic phase of infection.

3.2. Ucp2 expression following infection detected by Northern blot

Fig. 2 illustrates Northern blot analysis showing the *Ucp2* expression in the mouse brain following infection with *T. gondii*. Total RNA extracts were obtained from control mice, infected G at day 28 and infected NG at day 28. *Ucp2* mRNA was normalized to 18 S. Chronic infection with *T. gondii* led to a significant increase in the *Ucp2* expression (respectively, 240% and 410% for G and NG, $p < 0,001$, $n = 3$).

We have tried different antibodies against brain *Ucp2* but none proved to be suitable as we and our collaborators (Pecqueur et al., 2001) and others (Nishio et al., 2005) have shown that antibodies to *Ucp2* protein reacts in a tissue specific manner. No suitable antibody was found for brain *Ucp2* as they either gave more than one band or could not be detected by Western blot from brain extracts. Therefore we could not do any double labeling experiments with *Ucp2* protein. However, a role for *Ucp2* in brain neuroprotection has been shown using *Ucp2* transgenic mice (Mattiasson et al., 2003) and *Ucp2* KO mice (de Bilbao et al., 2004). In addition, *Ucp2* KO mice have altered appetite control following MCAO (Arsenijevic et al., 2006). A transgenic *Ucp2* mouse strain has also been shown to modify NPY brain levels associated with increased food intake (Horvath et al., 2003).

3.3. Distribution of Ucp2 mRNA throughout the brain of mice chronically infected with T. gondii

To determine in which nuclei the expression of *Ucp2* was enhanced, we used *in situ* hybridization on brain from mice at different times following the infection. The rostrocaudal distribution of *Ucp2* mRNA in the brains of control mice and of mice after 3, 9, and 28 (NG and G) days post-infection is illustrated in Fig. 3. Under basal conditions, the expression of *Ucp2* was found in several regions of the brain. The hybridization signal was strong in hypothalamic nuclei that include the median preoptic nucleus, suprachiasmatic nucleus, paraventricular hypothalamic nucleus, ARC, VMH, and dorsomedial hypothalamic nucleus. Also, others regions of the forebrain such as the septal region, amygdala and thalamus all expressed significant levels of *Ucp2* mRNA. In the thalamus, the expression was especially strong in the submedius thalamic nucleus [for a complete distribution, see (Richard et al., 1998)].

The distribution of the *Ucp2* transcript in the brain did not significantly change during the first three days following the infection with *T. gondii* (Day 1, data not shown). However, on day 9 and in the chronic stages of the infection, *Ucp2* expression augmented compared to controls. Also, the distribution of *Ucp2* was markedly different in infected mice
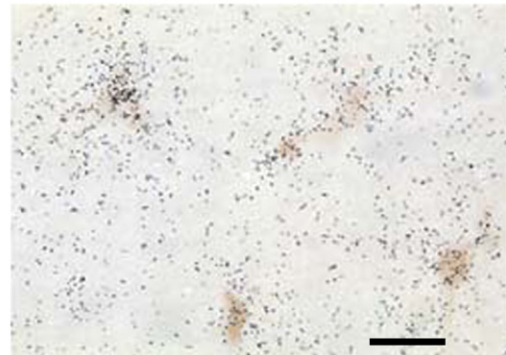
http://doc.rero.ch
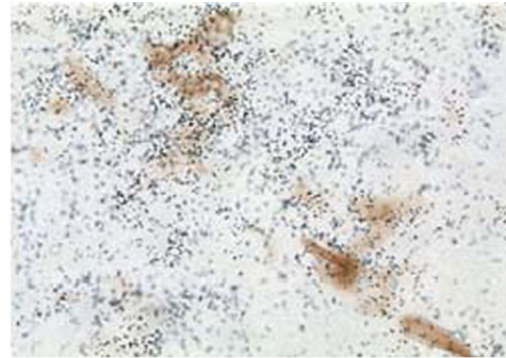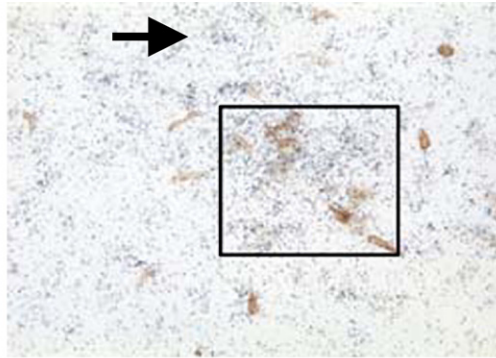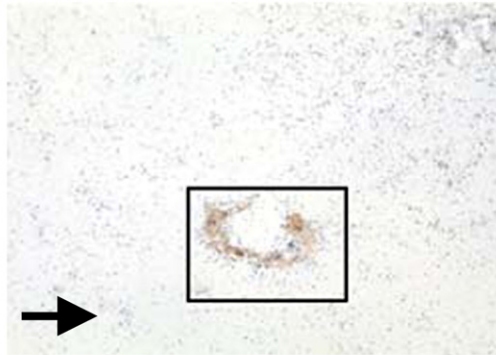
Fig. 5. Brightfield photomicrographs showing the type of cells expressing *Ucp2* mRNA in mice chronically infected with *Toxoplasma gondii* in the cerebral cortex, although inflammation was generalized throughout the brain. Neutrophils were labeled by immunocytochemistry using an anti-neutrophils antibody (upper panel), macrophages–monocytes cells were detected using F480 antibody (middle panel), while cells of myeloid origin were detected using an antibody directed against the iba1 molecule (lower panel). *Ucp2* mRNA was revealed by silver grains in cells, also note that in the different antibody stained immune cells sections there are areas of non-colored intense silver grains these are microglia. Microglial cells represent the majority of cells that were colocalized with *Ucp2* in the chronic phase of infection and are indicated by arrows in neutrophil and macrophage stain sections. Scale bar 7 μm.

compared to non-infected controls. Infection resulted in the presence of many areas giving a high signal and this was not associated with a given neuronal loci unlike what is characteristically seen in control mice (Fig. 3). Infection induced labeling that was associated with immune cell infiltration and the labeling also appeared around blood vessels.

The parasite load in the brain of G is less than in NG and is associated with a higher immune activation in the latter group (Arsenijevic et al., 1997). Concerning the intact cyst, we did not observe any co-association with *Ucp2* mRNA induced expression and inflammation loci, since most of the cysts were in neurons. The expression of *Ucp2* was associated with microglia and/or infiltrating immune cells, the later being believed to accumulate in response to the rupture of cysts

(Frenkel and Escajadillo, 1987). We did not observed that there was a specific brain site associated with cysts and/or inflammatory loci in the G or NG as cysts location and inflammatory loci appeared to be random. We did not found histological evidence for a link between inflammatory cells or cysts and specific regions involved in energy balance (hypothalamus or brain stem). The effect of infection and inflammation on neuronal energy balance centers therefore did not appear to be site specific.

We studied the mRNA levels of *Ucp2* in the AP, NST, ARC and VMH as examples of nuclei known to be involved in energy balance on day 3, 9 and 28 (for the latter in G and NG subgroups). As it can be seen from the results in Fig. 4, significant changes occurred in *Ucp2* levels in these areas after
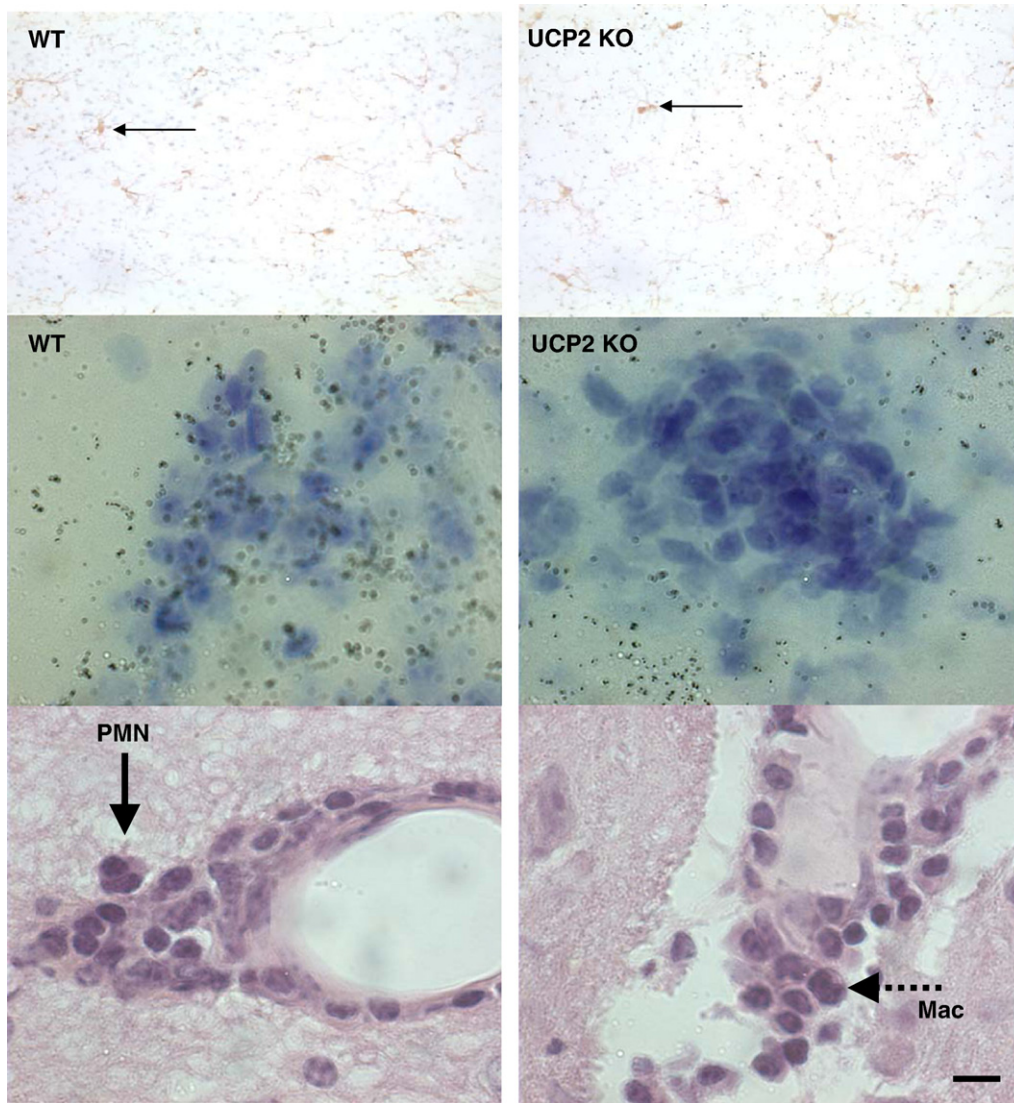
Fig. 6. *Ucp2 in situ* hybridization (black spots) and immunostained microglia with iba1 (brown colored cell indicated with arrow) in wild-type (WT) and infected *Ucp2* KO mice, this shows that microglia are still present in the *Ucp2* KO brain (upper 2 panels). *Ucp2 in situ* hybridization in infected wild-type (WT) and infected *Ucp2* KO mice (middle 2 panels) shows that in the brain of WT immune infiltrate inflammation loci there labeling of *Ucp2*, in marked contrast the immune infiltrates in *Ucp2* KO mice show no labeling. Morphological identification of infiltrating immune cells, neutrophils (PMN) are identified by their multi-lobed nuclei (arrow) and macrophage by their bean shaped nuclei (arrow), brain slices were stained with haemotoxylin and eosin. Scale bar7 μm.

infection. In particular, *Ucp2* in the AP and VMH was initially reduced following infection and then there was a gradual return near control levels in the NG only after 28 days of infection. In the NST, infection results in increases in *Ucp2*, which was maintained at significantly higher levels over the whole period of infection. In the ARC *Ucp2* was markedly reduced on day 9 after infection but in the early and later phases of infection it was similar to control levels.

3.4. Immune cells expression and double labeling with Ucp2

To characterize the immune cells infiltration time course and to verify which cell type expresses *Ucp2*, we used a double labeling procedure. During the first 3 days of infection, no lymphocyte of the CD45, CD45R, CD4 or CD8 subgroups, neutrophil, nor macrophages where seen in the brain. At the same time, the brain microglial cells were activated, as evidenced by F4/80 staining and reconfirmed with Iba staining, but this was not associated with the induction of *Ucp2* in the those cells (data not shown). Progression of the infection resulted in an increase in *Ucp2* mRNA. This was associated with increased lymphocyte invasion in blood vessels, ventricle spaces and brain tissue. Immunohistochemistry and double labeling with *Ucp2* identified neutrophils (Fig. 5, upper panel) and macrophages (Fig. 5, middle panel) to be the main cells to infiltrate the brain parenchyma where *Ucp2* expression was increased at day 14. Further colocalization with mRNA and cell type revealed that most of the *Ucp2* was associated with activated microglial cells in brain inflammation sights (Fig. 5, lower panel). Macrophages also expressed *Ucp2* in high quantities but appeared less frequent than microglial cells in brain tissue. However, they were the major source of *Ucp2* in
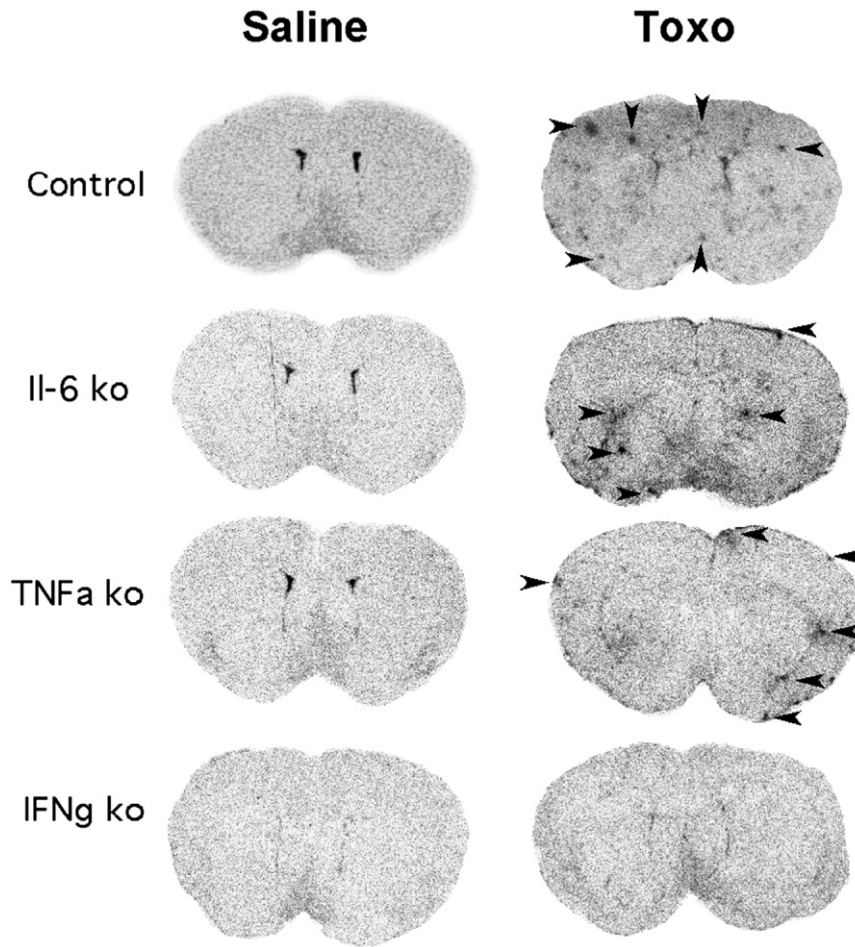
7

Saline **Toxo**

Fig. 7. Central *Ucp2* expression in IL-6 KO, TNF-α KO and IFN-γ KO mice at day 9 following *Toxoplasma gondii* infection. The pictures represent the X-ray film autoradiograms of coronal brain sections that were hybridized with an antisense riboprobe complementary to mouse *Ucp2* mRNA. Each presented section approximately corresponds to the same rostrocaudal level, which allows the comparison between mice. Sections are representative of the expression obtained in each animals of a given group. Note the absence of enhanced *Ucp2* expression in IFN-γ KO mice as compared to the IL-6 KO and TNF-α KO mice (black arrows).

ventricular space and in blood vessels (Fig. 5, middle panel). Blood vessel endothelial cells as identified with von Will-abrandt Factor (vWF) showed variable expression of *Ucp2*. In fact, not all vWF positive blood vessels express *Ucp2* (not shown). Blood vessels in control animals were not observed to have elevated *Ucp2*. The variable expressions suggest differential activation or infiltration of other *Ucp2* positive cells. There was an association with immunocytochemical labeled neutrophils (Fig. 5, upper panel) and no association with natural killer cells, CD45R, CD45, CD8$^+$ and CD4$^+$ T cells (data not shown).

Ucp2 colocalization with microglial cells at day 9 and onward was surprising since activated microglial cells were found in the first days after infection but were not associated with an increased *Ucp2* expression. However, one important factor at day 9, which could have led to the induction of *Ucp2* was the invasion of immune cells in the areas of increased *Ucp2* expression and microglial activated cells. This suggests that immune cells (phagocytes and lymphocytes) may produce factors that are required for *Ucp2* induction. We show that *Ucp2* KO mice have microglia and the lack of *Ucp2* induction in these mice cannot be explained by the lack of these cells in

the brain (Fig. 6). Neutrophils, macrophage/monocytes and lymphocytes were not detected in the brains of non-infected controls and are therefore control slides are not shown. We show that immune infiltrates in wild-type mice show *Ucp2* staining where as brain immune cell infiltrates in *Ucp2* KO mice do not (Fig. 6). Immune cell infiltration morphological identification (neutrophils, macrophage/monocytes, lymphocytes) and colocalization with *Ucp2* (silver grains) was also carried out with histochemical staining with haematoxylin–eosin staining (Fig. 6).

3.5. Central Ucp2 expression in IL-6 KO, TNF-α KO and IFN-γ KO mice

Since *T. gondii* infection is associated with increased cytokines levels, we have used gene knockout mice for IL-6, TNF-α and IFN-γ in order to examine the role of these important cytokines in toxoplasmosis and the expression of *Ucp2* in microglia. We chose those three cytokines because they are the in the brain of chronically infected mice and are produced by macrophages and/or lymphocytes. Toxoplasmosis results in an increase expression of *Ucp2* compared to saline-

injected controls in the IL-6 KO and TNF-α KO mice 9 days after treatment (Fig. 7 middle panels). However, in the IFN-γ KO mice, enhanced microglial *Ucp2* expression was not observed following 9 days of infection (Fig. 7, lower panel). This suggests that IFN-γ is an important factor in the *Ucp2* induction following toxoplasmosis in microglia.

4. Discussion

The present study demonstrates that global brain *Ucp2* expression is enhanced during chronic toxoplasmosis as measured by northern blot. This observation was confirmed by *in situ* hybridization and this method allowed us to show that the distribution of *Ucp2* was markedly altered following infection. We observed a shift in the cellular sites of expression of *Ucp2*, initially from neurons to blood vessels and cellular inflammation clusters. In the acute phase, there was no difference in the cellular pattern of *Ucp2* expression compared to non-infected controls; it was in neurons and in cells lining the brain. From day 9 post-infection, we found that *Ucp2* colocalizes along with macrophages/monocytes and neutrophils that had infiltrated into brain tissue. However, a certain proportion of *Ucp2* mRNA from this time on was associated with activated microglia as indicated by F4/80 staining. This finding is somewhat surprising since activated microglial cells were detected 3 days after infection but there was no associated increase in *Ucp2* expression. One significant difference between early microglia on day 1 and 3 post-infection compared to day 9 is the presence of brain immune cell infiltration, in particular lymphocytes and blood phagocytes in areas of microglial activated cells with increased *Ucp2* expression at the later time point. This suggests that *Ucp2* in microglial cells cannot be directly induced by factors released from other microglial cells, astrocytes, neurons and brain blood vessel cells but require the presence immune cells (lymphocytes, macrophage, neutrophils) or substances released by these cells to induce microglial *Ucp2* in this model.

We also demonstrate for the first time that *Ucp2* is expressed at high levels in neutrophils. This is of particular importance since neutrophils are considered to be the phagocytes that produce the most ROS by the NADPH oxidase when they come into contact with foreign agents or during infection. Neutrophils are known to usually have a low number of mitochondria and this may be due to the high amounts of ROS that these cells are potentially capable of producing, which could in turn be toxic to mitochondria (Fossati et al., 2003).

ROS may originate from many different sources including mitochondria, peroxisomes, microsomes and by oxidases, and the importance of these sources may vary depending whether it is under basal conditions or during a stress or an inflammatory process (Droge, 2002; Fang et al., 2002). In particular during inflammation or infection, cells such as neutrophils, macrophages, microglia and other phagocytes, which are important in innate defenses, can produce a lot of ROS by the NADPH oxidase system (Victor et al., 2004) to eliminate microbes. Macrophages are capable of increasing *Ucp2* in relation to their capacity for respiratory burst (Nishio et al., 2005). The Nishio

study implies that *Ucp2* is strongly associated with the cells capacity to produce ROS and therefore supports a role for *Ucp2* as an anti-ROS regulator. A role for *Ucp2* to regulate NADPH oxidase at least at the protein level does not appear to be a mechanism (Nishio et al., 2005; Bai et al., 2005). *Ucp2* regulation of ROS could be due to altering ATP, NADPH and GSH levels, this could determine the redox state of a cell and its organelles (i.e. mitochondria). ATP, NADPH, GSH are linked by the synthesis of GSH an important anti-oxidant which can determine ROS levels (Li, 1999). *Ucp2*'s proposed role is to protect mitochondria from ROS since these organelles are vital for cell survival (Gibson and Huang, 2004). However the importance of mitochondrial ROS *vs* NADPH oxidase ROS in an anti-toxoplasmic activity must take into account that *T. gondii* has been show to have a close association with the host mitochondria (Sinai et al., 1997).

Evidence suggests that *Ucp2* could limit the production of ROS (Arsenijevic et al., 2000; Negre-Salvayre et al., 1997; Nicholls and Budd, 2000; Richard et al., 1998; Skulachev, 1998). Since macrophages and microglia can secrete ROS, it is plausible that the *Ucp2* over-expression in these cells may protect cells from free radical damage in the lesion sites. Accordingly, we recently showed that macrophages from *Ucp2* KO mice produce more ROS than wild-type mice, emphasizing a role for *Ucp2* in ROS production in phagocytes (Arsenijevic et al., 2000). Taking into account the temporal induction of *Ucp2* in brain microglial cells, this induction is probably not directly due to a general increase in oxidative stress but a specific local production, since it was shown that reactive oxygen species and lipid peroxidation already occurs by day 1 post-infection (Arsenijevic et al., 2001). However, ROS may indirectly activate *Ucp2* expression by depleting or inactivating some anti-oxidant systems (de Bilbao et al., 2004) and it is known that redox state can regulate gene expression. The anti-oxidant state of the cell or mitochondria in particular may regulate *Ucp2*. In a recent study using a murine model of cerebral ischemia, *Ucp2* was induced to a maximal levels only when mitochondrial glutathione was depleted and it may act as a GSH transporter (de Bilbao et al., 2004; Fernandez-Checa and Kaplowitz, 2005).

Cytokines are important regulators of ROS and in particular IFN-γ. In our model, the induction of *Ucp2* in the microglia seems to be largely dependent on IFN-γ since the IFN-γ KO mice did not exhibit any enhanced expression in the parenchyma. The increased induction of *Ucp2* mRNA in microglia does not seem to be regulated by IL-6 or TNF-α because the respective KO mice showed an increase *Ucp2* response to infection. Our result with TNF-α is in contrast to what has been observed in peripheral tissues such as liver (Cortez-Pinto et al., 1998; Faggioni et al., 1998), muscle (Busquets et al., 1998; Faggioni et al., 1998), white adipose tissue (Faggioni et al., 1998) and heart (Noma et al., 2001) where TNF-α induced *Ucp2* expression. However, our finding is consistent with another study showing that the effect of an acute treatment of LPS on the *Ucp2* expression in the brain was not mediated by TNF-α (Busquets et al., 2001). This suggests that TNF-α may have an indirect effect on *Ucp2* induction

depending on the tissue or cell involved in *Ucp2* expression. It should be remembered that TNF-α is also capable of acutely upregulating IFN-γ (Car et al., 1994) so some of the observed effects of TNF-α may be due to cytokines it induces.

Our findings support previous studies in that the induction of *Ucp2* occurs in different tissues following immune activation (Busquets et al., 2001; Cortez-Pinto et al., 1998; Faggioni et al., 1998; Lee et al., 1999; Masaki et al., 1999; Yu et al., 2000). These results are consistent with the proposition that *Ucp2* upregulation by LPS and other cytokines reported using Northern blots may in part be regulated by immune cell infiltration (Busquets et al., 2001; Faggioni et al., 1998; Yu et al., 2000). Recent studies by our group have demonstrated that *Ucp2* gene expression can be induced in neuronal as well as in microglial cells following exposure to kainic acid or in cerebral ischemia (Clavel et al., 2003; de Bilbao et al., 2004). It should be noted that the kainic acid-induced *Ucp2* does not involve infiltrating immune cells. This suggests that different factors regulate *Ucp2* in different cell types. We further show that following toxoplasmosis, *Ucp2* regulation in neurons differs from that in microglia.

Our study also demonstrates that *Ucp2* is markedly decreased in the AP and the VMH whereas it is increased in the NST on day three post-infection. This indicates that neuronal *Ucp2* changes can occur in the absence of immune cell infiltration in the CNS unlike microglia. It is not known whether the modified neuronal *Ucp2* expression is due to factors external or internal to the brain. It should be noted that in our model there is an increase in the oxidative stress in the brain following infection before the observed immune cell infiltration and it may be this oxidative stress that alters *Ucp2* (Arsenijevic et al., 2001).

The major role proposed for *Ucp2* has been that it regulates ROS production (Negre-Salvayre et al., 1997; Arsenijevic et al., 2000), however other studies suggest that it may regulate insulin secretion (Kassis et al., 2001; Zhang et al., 2001). *T. gondii* infection results in induction of *Ucp2* mRNA in the chronic phase of infection in various tissues (muscle, white adipose tissue, brown adipose tissue, pancreas — data not shown). The observed increased pancreatic *Ucp2* in infected mice was associated with a decrease in plasma insulin levels in chronically infected mice (Picard et al., 2002). This is consistent with other studies suggesting that *Ucp2* is a negative regulator of insulin secretion (Zhang et al., 2001).

There is evidence of *Ucp2* chromosomal location with genetic linkage to obesity (Fleury et al., 1997). Initial studies with *Ucp2* KO mice did not show evidence that there was food intake or energy expenditure differences between KO and WT mice under basal conditions (Arsenijevic et al., 2000). However complementary adaptation may have occurred in the KO mice, since food intake regulation and energy expenditure are regulated in a composite nature. For example following cerebral ischemia *Ucp2* KO mice have compensated activation of anti-oxidant mechanisms in the basal state prior to brain injury (de Bilbao et al., 2004). We have shown that *Ucp2* KO mice have altered food intake responses following cerebral ischemia with an implication of neuropeptide Y (NPY) (Arsenijevic et al., 2006). *Ucp2* transgenic mice have increased food intake and

this was associated also with NPY levels (Horvath et al., 2003). Furthermore *Ucp2* is found in areas where NPY has been localized (Lin et al., 2006; Glass et al., 2002). NPY may also influence other homeostasis mechanisms apart from food intake such as corticosterone, thyroid status and other neuroendocrine hormones (Harfstrand, 1987). In particular corticosterone and thyroid hormones are altered in toxoplasmosis (Picard et al., 2002; Stahl and Kaneda, 1998). Toxoplasmosis results in cachexia and a possible role for the VMH is suggested since this brain site is involved in catabolic responses (Uyama et al., 2004). One would expect differences in nuclei activation between G and NG since G are hypophagic whereas NG are hypophagic and hypermetabolic. Our finding of altered *Ucp2* mRNA levels in neurons suggest when integrating the above information that *Ucp2* may regulate energy balance pathways. Our study indicates that *Ucp2* may do more than just regulate ROS.

The association of *Ucp2* in the NST and the degree of body weight loss also supports the notion that *Ucp2* in neurons may be involved in energy food intake responses following central inflammation (Arsenijevic et al., 2006). If *Ucp2* was only regulating ROS then one would expect that neuronal *Ucp2* would increase rather than decrease after infection. Furthermore one would not expect *Ucp2* in one group of neurons to increase while it decreases in another group at the same time after infection. This study suggests that *Ucp2* may have other functions than ROS regulation. It may be involved in energy balance *via* a cell-specific neuronal regulation. Further studies of *Ucp2* in neurons involved in energy balance are required to elucidate whether *Ucp2* alters neuronal energy balance homeostatic pathway signalling as this study suggests.

5. Conclusions

Using our model of murine toxoplasmosis we were able to demonstrate that *Ucp2* mRNA regulation is a complex process in the brain following infection. Our study suggests that *Ucp2* mRNA is regulated in a different manner in neurons than in brain phagocytes. The former do not appear to require presence of infiltrating immune cells whereas the latter do. Increased *Ucp2* levels are associated with negative energy balance. We show that *Ucp2* expression in certain nuclei associated with energy balance such as the NTS follow changes in energy balance following infections whereas other nuclei do not. The case for NTS *Ucp2* nuclei regulating energy balance is implicated by a temporal association, this further supports our previous data that *Ucp2* is implicated in energy balance during inflammation (Arsenijevic et al., 2006). Due to the unexpected increase or decrease in different nuclei at the same moment in time we conclude that *Ucp2* may not only directly be regulating oxidative stress. *Ucp2* may regulate cell function by oxidative stress sensing which may involve changes in mitochondrial glutathione levels as we have previously suggested. In particular for future studies it would be interesting to study the changes of *Ucp2* and their association with changes in expression of neuropeptides in these different nuclei involve in neuroendocrine regulation of homeostasis.

References

Andrews, Z.B., Horvath, B., Barnstable, C.J., Elseworth, J., Yang, L., Beal, M.F., Roth, R.H., Matthews, R.T., Horvath, T.L., 2005. Uncoupling protein-2 is critical for nigral dopamine cell survival in a mouse model of Parkinson's disease. J. Neurosci. 25, 184–191.

Argyropoulos, G., Harper, M.E., 2002. Uncoupling proteins and thermoregulation. J. Appl. Physiol. 92, 2187–2198.

Arsenijevic, D., Girardier, L., Seydoux, J., Chang, H.R., Dulloo, A.G., 1997. Altered energy balance and cytokine gene expression in a murine model of chronic infection with *Toxoplasma gondii*. Am. J. Physiol. 272, E908–E917.

Arsenijevic, D., Onuma, H., Pecqueur, C., Raimbault, S., Manning, B.S., Miroux, B., Couplan, E., Alves-Guerra, M.C., Goubern, M., Surwit, R., Bouillaud, F., Richard, D., Collins, S., Ricquier, D., 2000. Disruption of the uncoupling protein-2 gene in mice reveals a role in immunity and reactive oxygen species production. Nat. Genet. 26, 435–439.

Arsenijevic, D., de Bilbao, F., Giannakopoulos, P., Girardier, L., Samec, S., Richard, D., 2001. A role for interferon-gamma in the hypermetabolic response to murine toxoplasmosis. Eur. Cytokine Netw. 12, 518–527.

Arsenijevic, D., de Bilbao, F., Plamondon, J., Paradis, E., Vallet, P., Richard, D., Langhans, W., Giannakopoulos, P., 2006. Increased infarct size and lack of hyperphagic response after focal cerebral ischemia in peroxisome proliferator-activated receptor-beta-deficient mice. J. Cereb. Blood Flow Metab. 263, 433–445.

Bai, Y., Onuma, H., Bai, X., Medvedev, A.V., Misukonis, M., Weinberg, J.B., Cao, W., Robidoux, J., Floering, L.M., Daniel, K.W., Collins, S., 2005. Persistent nuclear factor-kB activation in Ucp2−/− mice leads to enhanced nitric oxide and inflammatory cytokine production. J. Biol. Chem. 280, 18063–18069.

Busquets, S., Sanchis, D., Alvarez, B., Ricquier, D., Lopez-Soriano, F.J., Argiles, J.M., 1998. In the rat, tumor necrosis factor alpha administration results in an increase in both UCP2 and UCP3 mRNAs in skeletal muscle: a possible mechanism for cytokine-induced thermogenesis? FEBS Lett. 440, 348–350.

Busquets, S., Alvarez, B., Van Royen, M., Figueras, M.T., Lopez-Soriano, F.J., Argiles, J.M., 2001. Increased uncoupling protein-2 gene expression in brain of lipopolysaccharide-injected mice: role of tumour necrosis factor-alpha? Biochim. Biophys. Acta 1499, 249–256.

Car, B.D., Eng, V.M., Schnyder, B., Ozmen, L., Huang, S., Gallay, P., Heumann, D., Aguet, M., Ryffel, B., 1994. Interferon gamma receptor deficient mice are resistant to endotoxic shock. J. Exp. Med. 179, 1437–1444.

Chao, C.C., Hu, S., Gekker, G., Novick Jr., W.J., Remington, J.S., Peterson, P.K., 1993. Effects of cytokines on multiplication of *Toxoplasma gondii* in microglial cells. J. Immunol. 150, 3404–3410.

Chomczynski, P., Sacchi, N., 1987. Single-step method of RNA isolation by acid guanidinium thiocyanate–phenol–chloroform extraction. Anal. Biochem. 162, 156–159.

Clavel, S., Paradis, E., Ricquier, D., Richard, D., 2003. Kainic acid upregulates uncoupling protein-2 mRNA expression in the mouse brain. NeuroReport 14, 2015–2017.

Cortez-Pinto, H., Yang, S.Q., Lin, H.Z., Costa, S., Hwang, C.S., Lane, M.D., Bagby, G., Diehl, A.M., 1998. Bacterial lipopolysaccharide induces uncoupling protein-2 expression in hepatocytes by a tumor necrosis factor-alpha-dependent mechanism. Biochem. Biophys. Res. Commun. 251, 313–319.

Daubener, W., Hadding, U., 1997. Cellular immune reactions directed against *Toxoplasma gondii* with special emphasis on the central nervous system. Med. Microbiol. Immunol. (Berl) 185, 195–206.

de Bilbao, F., Arsenijevic, D., Vallet, P., Hjelle, O.P., Ottersen, O.P., Bouras, C., Raffin, Y., Abou, K., Langhans, W., Collins, S., Plamondon, J., Alves-Guerra, M.C., Haguenauer, A., Garcia, I., Richard, D., Ricquier, D., Giannakopoulos, P., 2004. Resistance to cerebral ischemic injury in UCP2 knockout mice: evidence for a role of UCP2 as a regulator of mitochondrial glutathione levels. J. Neurochem. 89, 1283–1292.

Diano, S., Matthews, R.T., Patrylo, P., Yang, L., Beal, M.F., Barnstable, C.J., Horvath, T.L., 2003. Uncoupling protein 2 prevents neuronal death including that occurring during seizures: a mechanism for preconditioning. Endocrinology 144, 5014–5021.

Droge, W., 2002. Free radicals in the physiological control of cell function. Physiol. Rev. 82, 47–95.

Echtay, K.S., Roussel, D., St-Pierre, J., Jekabsons, M.B., Cadenas, S., Stuart, J.A., Harper, J.A., Roebuck, S.J., Morrison, A., Pickering, S., Clapham, J.C., Brand, M.D., 2002. Superoxide activates mitochondrial uncoupling proteins. Nature 415, 96–99.

Faggioni, R., Shigenaga, J., Moser, A., Feingold, K.R., Grunfeld, C., 1998. Induction of UCP2 gene expression by LPS: a potential mechanism for increased thermogenesis during infection. Biochem. Biophys. Res. Commun. 244, 75–78.

Fang, Y.Z., Yang, S., Wu, G., 2002. Free radicals, antioxidants and nutrition. Nutrition 18, 872–879.

Fernandez-Checa, J.C., Kaplowitz, N., 2005. Hepatic mitochondrial glutathione: transport and role in disease and toxicity. Toxicol. Appl. Pharmacol. 204, 263–273.

Fleury, C., Sanchis, D., 1999. The mitochondrial uncoupling protein-2: current status. Int. J. Biochem. Cell Biol. 31, 1261–1278.

Fleury, C., Neverova, M., Collins, S., Raimbault, S., Champigny, O., Levi-Meyrueis, C., Bouillaud, F., Seldin, M.F., Surwit, R.S., Ricquier, D., Warden, C.H., 1997. Uncoupling protein-2: A novel gene linked to obesity and hyperinsulinaemia. Nat. Genet. 15, 269–272.

Fossati, G., Moulding, D.A., Spiller, D.G., Moots, R.J., White, M.R.H., Edwards, S.W., 2003. The mitochondrial network of human neutrophils: role in chemotaxis, phagocytosis, respiratory burst activation and commitment to apoptosis. J. Immunol. 170, 1964–1972.

Frenkel, J.K., Escajadillo, A., 1987. Cyst rupture as a pathogenic mechanism of toxoplasmic encephalitis. Am. J. Trop. Med. Hyg. 36, 517–522.

Gibson, G.E., Huang, H.M., 2004. Mitochondrial enzymes and endoplasmic reticulum calcium stores as targets of oxidative stress in neurodegenerative diseases. J. Bioenerg. Biomembranes 36, 335–340.

Glass, M.J., Chan, J., Pickel, V.M., 2002. Ultrastructural localization of neuropeptide Y Y1 receptors in the rat medial nucleus tractus solitarius: relationship with neuropeptide Y or catecholamine neurons. J. Neurosci. Res. 67, 753–765.

Harfstrand, A., 1987. Brain neuropeptide Y mechanisms. Basic aspects and involvement in cardiovascular and endocrine regulation. Acta Physiol. Scand., Suppl. 565, 1–83.

Holliman, R.E., Greig, L., 1997. Toxoplasmosis in immunocompromised patients. Curr. Opin. Infect. Dis. 10, 281–284.

Horvath, T.L., Diano, S., Miyamoto, S., Barry, S., Gatti, S., Alberati, D., Livak, F., Lombardi, A., Moreno, M., Goglia, F., Mor, G., Hamilton, J., Kachinaskas, D., Horwitz, B., Warden, C.H., 2003. Uncoupling proteins-2 and 3 influence obesity and inflammation in transgenic mice. Int. J. Obes. 27, 433–442.

Kassis, N., Bernard, C., Pusterla, A., Casteilla, L., Penicaud, L., Richard, D., Ricquier, D., Ktorza, A., 2001. Correlation between pancreatic islet uncoupling protein-2 (UCP2) mRNA concentration and insulin status in rats. Int. J. Exp. Diabetes Res. 1, 185–193.

Lee, F.Y., Li, Y., Zhu, H., Yang, S., Lin, H.Z., Trush, M., Diehl, A.M., 1999. Tumor necrosis factor increases mitochondrial oxidant production and induces expression of uncoupling protein-2 in the regenerating mice [correction of rat] liver. Hepatology 29, 677–687.

Li, S.C., 1999. Regulation of hepatic glutathione synthesis: current concepts and controversies. FASEB J. 13, 1169–1183.

Lin, S., Boey, D., Lee, N., Schwarzer, C., Sainsbury, A., Herzog, H., 2006. Distribution of prodynorphin mRNA and its interaction with the NPY system in the mouse brain. Neuropeptides 40, 115–123.

Masaki, T., Yoshimatsu, H., Kakuma, T., Chiba, S., Hidaka, S., Tajima, D., Kurokawa, M., Sakata, T., 1999. Induction of rat uncoupling protein-2 gene treated with tumour necrosis factor alpha in vivo. Eur. J. Clin. Investig. 29, 76–82.

Mattiasson, G., Shamloo, M., Gido, G., Mathi, K., Tomasevic, G., Yi, S., Warden, C.H., Castilho, R.F., Melcher, T., Gonzalez-Zulueta, M., Nikolich, K., Wieloch, T., 2003. Uncoupling protein-2 prevents neuronal death and diminishes brain dysfunction after stroke and brain trauma. Nat. Med. 9, 1062–1068.

Mizuno, T., Miura-Suzuki, T., Yamashita, H., Mori, N., 2000. Distinct regulation of brain mitochondrial carrier protein-1 and uncoupling protein-

2 genes in the rat brain during cold exposure and aging. Biochem. Biophys. Res. Commun. 278, 691–697.

Negre-Salvayre, A., Hirtz, C., Carrera, G., Cazenave, R., Troly, M., Salvayre, R., Penicaud, L., Casteilla, L., 1997. A role for uncoupling protein-2 as a regulator of mitochondrial hydrogen peroxide generation. FASEB J. 11, 809–815.

Nicholls, D.G., Budd, S.L., 2000. Mitochondria and neuronal survival. Physiol. Rev. 80, 315–360.

Nichols, D.G., Locke, R.M., 1984. Thermogenic mechanisms in brown fat. Physiol. Rev. 64, 1–64.

Nishio, K., Qiao, S., Yamashita, H., 2005. Characterisation of differential expression of uncoupling protein 2 and ROS production in differential mouse macrophage-cells (Mm1) and progenitor cells (M1). J. Mol. Histol. 36, 35–44.

Noma, T., Nishiyama, A., Mizushige, K., Murakami, K., Tsuji, T., Kohno, M., Rahman, M., Fukui, T., Abe, Y., Kimura, S., 2001. Possible role of uncoupling protein in regulation of myocardial energy metabolism in aortic regurgitation model rats. FASEB J. 15, 1206–1208.

Pecqueur, C., Alves-Guerra, M., Gelly, C., Levi-Meyrueis, C., Couplan, E., Collins, S., Ricquier, D., Bouillaud, F., Miroux, B., 2001. Uncoupling protein-2 in vivo distribution, induction upon oxidative stress and evidence for translational regulation. J. Biol. Chem. 276, 8706–8712.

Picard, F., Arsenijevic, D., Richard, D., Deshaies, Y., 2002. Response of adipose and muscle lipoprotein lipase to chronic infection and subsequent acute lipopolysaccharide challenge. Clin. Diagn. Lab. Immunol. 9, 771–776.

Richard, D., Rivest, R., Huang, Q., Bouillaud, F., Sanchis, D., Champigny, O., Ricquier, D., 1998. Distribution of the uncoupling protein 2 mRNA in the mouse brain. J. Comp. Neurol. 397, 549–560.

Ricquier, D., Bouillaud, F., 2000. Mitochondrial uncoupling proteins: from mitochondria to the regulation of energy balance. J. Physiol. 529 (Pt 1), 3–10.

Simmons, D.M., Arriza, J.L., Swanson, L.W., 1989. A complete protocol for in situ hybridization of messenger RNAs in brain and other tissues with radiolabeled single-probe. J. Histotechnol. 12, 169–181.

Sinai, A.P., Webster, P., Joiner, K.A., 1997. Association of host cell endoplasmic reticulum and mitochondria with the *Toxoplasma gondii* parasitophorous vacuole membrane: a high affinity interaction. J. Cell Sci. 110, 2117–2122.

Skulachev, V.P., 1998. Uncoupling: new approaches to an old problem of bioenergetics. Biochim. Biophys. Acta 1363, 100–124.

Stahl, W., Kaneda, Y., 1998. Impaired thyroid dysfunction in murine toxoplasmosis. Parasitology 117, 217–222.

Sullivan, P.G., Dube, C., Dorenbos, K., Steward, O., Baram, T.Z., 2003. Mitochondrial uncoupling protein-2 protects the immature brain from excitotoxic neuronal death. Ann. Neurol. 53, 711–717.

Uyama, N., Geerts, A., Reynaert, H., 2004. Neural connections between hypothalamus and the liver. Anat. Rec. A Discov. Mol. Cell. Evol. Biol. 280A, 8080–8820.

Victor, V.M., Rocha, M., De la Fuente, M., 2004. Immune cells: free radicals and antioxidants in sepsis. Int. Immunopharmacol. 4, 327–347.

Yap, G.S., Sher, A., 1999. Cell-mediated immunity to *Toxoplasma gondii*: initiation, regulation and effector function. Immunobiology 201, 240–247.

Yu, X.X., Barger, J.L., Boyer, B.B., Brand, M.D., Pan, G., Adams, S.H., 2000. Impact of endotoxin on UCP homolog mRNA abundance, thermoregulation, and mitochondrial proton leak kinetics. Am. J. Physiol., Endocrinol Metabol. Gastrointest. Physiol. 279, E433–E446.

Zhang, C.Y., Baffy, G., Perret, P., Krauss, S., Peroni, O., Grujic, D., Hagen, T., Vidal-Puig, A.J., Boss, O., Kim, Y.B., Zheng, X.X., Wheeler, M.B., Shulman, G.I., Chan, C.B., Lowell, B.B., 2001. Uncoupling protein-2 negatively regulates insulin secretion and is a major link between obesity, beta cell dysfunction, and type 2 diabetes. Cell 105, 745–755.